Applied Biochemistry and Biotechnology (2024) 196:4256–4272
https://doi.org/10.1007/s12010-023-04756-8

ORIGINAL ARTICLE

Biomechanical Scaffolds of Decellularized Heart Valves Modified by Electrospun Polylactic Acid

Chaorong Wang[1] · Qingqing Chen[1] · Han Wang[2,3] · Hanlin Gang[1] · Yingshan Zhou[1] · Shaojin Gu[1] · Ruoyun Zhang[1] · Weilin Xu[2] · Hongjun Yang[1,2]

Accepted: 17 October 2023 / Published online: 3 November 2023

Abstract

Enhancing the mechanical properties and cytocompatibility of decellularized heart valves is the key to promote the application of biological heart valves. In order to further improve the mechanical properties, the electrospinning and non-woven processing methods are combined to prepare the polylactic acid (PLA)/decellularized heart valve nanofiber-reinforced sandwich structure electrospun scaffold. The effect of electrospinning time on the performance of decellularized heart valve is investigated from the aspects of morphology, mechanical properties, softness, and biocompatibility of decellularized heart valve. Results of the mechanical tests show that compared with the pure decellularized heart valve, the mechanical properties of the composite heart valve were significantly improved with the tensile strength increasing by 108% and tensile strain increased by 571% when the electrospinning time exceeded 2 h. In addition, with this electrospinning time, the composite heart valve has a certain promoting effect on the human umbilical vein endothelial cells proliferation behavior. This work provides a promising foundation for tissue heart valve reendothelialization to lay the groundwork for organoid.

Keywords Heart valve · Electrospun scaffold · Sandwich composite structure · Biomechanics · Artificial heart valve

✉ Ruoyun Zhang
ryzhang@wtu.edu.cn

✉ Hongjun Yang
h_j.yang@yahoo.com

[1] College of Materials Science and Engineering, Wuhan Textile University, No.1 Yangguang Road, Wuhan 430200, Hubei Province, China

[2] State Key Laboratory of New Textile Materials and Advanced Processing Technologies, Wuhan Textile University, Wuhan 430200, China

[3] Institute for Frontier Materials, Deakin University, Geelong, Victoria 3216, Australia

Introduction

More than 200 thousand heart valve replacements are performed worldwide each year, with a predicted increment to 850 thousand by 2050 [1]. Heart valve replacement is needed when the heart valve is defective, narrowed, or with a lesion, which leads to abnormal heart function and heart failure [2].

In clinical heart valve replacement, bioprosthetic valve and mechanical valve are the most common prostheses. Despite the lifelong durability of mechanical valve, the patients need to bear considerable intraoperative and postoperative bleeding risk and take vitamin K antagonists regularly after heart valve replacement [3]. Compared with mechanical valves, bioprosthetic valves have a lower rate of thrombosis contributing to the needless lifelong anticoagulation of patients [4]. However, structural heart valve deterioration (SVD) of the implanted heart valve may appear between 10 and 15 years after surgery, which is especially concerned in young, low-risk patients with a long-life expectancy [5]. Therefore, bioprosthetic valves have limited durability leading to the long-term repeated heart valve replacements. All above cause great harm and risk to patients, so tissue-engineered heart valves (TEHV) with characteristics of growth have been widely investigated [6].

There are two approaches of tissue engineering: [1] in vitro—autologous or allogeneic cells are isolated and seeded on bioabsorbable scaffolds, then cultured in bioreactor systems until the new composite scaffold obtains sufficient mechanical elasticity and strength for implantation; [2] in situ—allogeneic or xenograft materials are decellularized for implantation to make cells grow and remodel the extracellular matrix (ECM) [7]. Decellular heart valve membrane (DHV) is one of the most frequent supporting materials in tissue engineering heart valves, as a stand-alone implant with the ability of recellularization in vivo due to the natural bioactive components, maintenance of the complex three-dimensional structure of the extracellular matrix, and splendid clinical relevance [8]. Biological scaffolds derived from natural tissues and organs are used in regenerative medicine for heart diseases in preclinical animal studies and clinical studies [9]. Typically, decellularized xenogeneic matrices involve the treatment of porcine or bovine tissue with detergents or enzymes to completely remove any of the cells to render it non-immunogenic with maintaining fiber orientation in the ECM [10–12], which were subsequently repopulated with autologous cells in vivo or in vitro [13]. Porcine heart valve is one of the biological scaffolds. The leaflets of the porcine heart valve are highly anisotropic, with radial elasticity almost four times stronger than the circumferential elasticity [14]. As shown in previous reports, porcine heart valve is an important research object [15, 16]. For example, Dai et al. combined degradable polyethylene glycol (PEG) hydrogel with decellularized porcine aortic heart valve to prepare a composite scaffold to promote the differentiation of bone marrow mesenchymal stem cells (BMSCs) into heart valve interstitial-like cells [17]. However, the decellularized porcine valve remains the problems of being hard to be stiffened and difficult to be processed.

The electrospinning technology has the powerful ability to create polymeric fiber networks with high surface area at the nanoscale by mimicking the extracellular matrix to provide more binding sites to cells [18]. In this regard, Del Gaudio et al. reported flexible electrospun PCL scaffolds for TEHVs in pediatric patients [19]. As we know, electrospun scaffolds have a natural extracellular matrix like that of natural valves and are widely used in tissue engineering, which can avoid the calcification problem caused by traditional glutaraldehyde treatment of heart valves to a certain extent. For another, the mechanical properties of electrospun scaffolds are comparable to those of natural valves, which can solve the problem of insufficient mechanical support caused

by hydrogels as scaffolds [20–22]. Therefore, PLA electrospun scaffolds are used in bone, cartilage, blood vessel, nerve, liver, kidney matrix, and drug delivery applications [23]. All in all, electrospinning membrane can provide certain mechanical support for decellularized heart valves as an ideal material for tissue engineering. However, since electrospinning is generally a fibrous membrane composed of hydrophobic polymers, it has poor hydrophilicity [24]. Therefore, compounding electrospun membrane with decellularized porcine valve attempts to address mechanical problems and obtain good hydrophilicity.

The sandwich structure enhanced the drain ability of cell flaps and polymer materials, as well as their overall mechanical qualities. The decellularized flap was both hydrophilic and mechanically weak; however, excessive hydrophilicity was not conducive to long-term scaffold support in the physiological fluid environment, and mechanical weakness would result in collapse when exposed to blood flow. To address the hydrophobic issue, a sandwich structure was created to improve the polymer's strong hydrophobicity while also increasing the hydrophilicity of the decellularized flap, resulting in an initial hydrophobic surface for cell adhesion. Following that, nutrition exchange and waste transfer take place around the decellularized flap to generate complete tissue, and when the PLA degrades, a tissue-engineered flap with tissue structure is formed. To improve the mechanical strength of the decellularized flap, which is mechanically weak and difficult to maintain in a straight state, a composite PLA electrostatic spinning membrane is used to enhance the overall mechanical strength of the composite flap scaffold with a sandwich structure to maintain uprightness under the action of blood flow. Therefore, the influence of the sandwich structure from the cellular valve composite polycystic acid on mechanical characteristics and drain ability is one of the breakthroughs of this work.

In this study, PLA and decellularized composite heart valve was prepared by the electrospinning process as raw materials with a sandwich structure electrospun scaffold (Fig. 1). On the one hand, the decellularized heart valve with a nanofibrous structure like native ECM obtained an extremely positive effect on cell behavior [25]. On the other hand, the decellularized heart valve provided a mechanical support layer in the middle. Furtherly, the PLA electrospun membrane on the surface improved the mechanical properties and compatibility of the PLA sandwich structure electrospun scaffold (PSES). The physicochemical properties of the scaffolds, cell viability, and behavior of human umbilical vein endothelial cells (HUVECs) demonstrated PSES had certain mechanical properties like strength and flexibility and good biocompatibility, which validated the potential as a biological valve scaffold.

Materials and Methods

Materials

PLA resin (6202D) with an average molecular weight of 97 kDa consisting of 98% L-lactide and 2% D-lactide units was purchased from NatureWorks LLC., USA. 1, 4-Dioxane was obtained from Sinopharm Chemical Reagent Co., Ltd. Dimethyl sulfoxide (DMSO) and dichloromethane (DCM) were purchased from Sinopharm Chemical Reagent Co., Ltd. All chemicals used in this work were analytical grade.

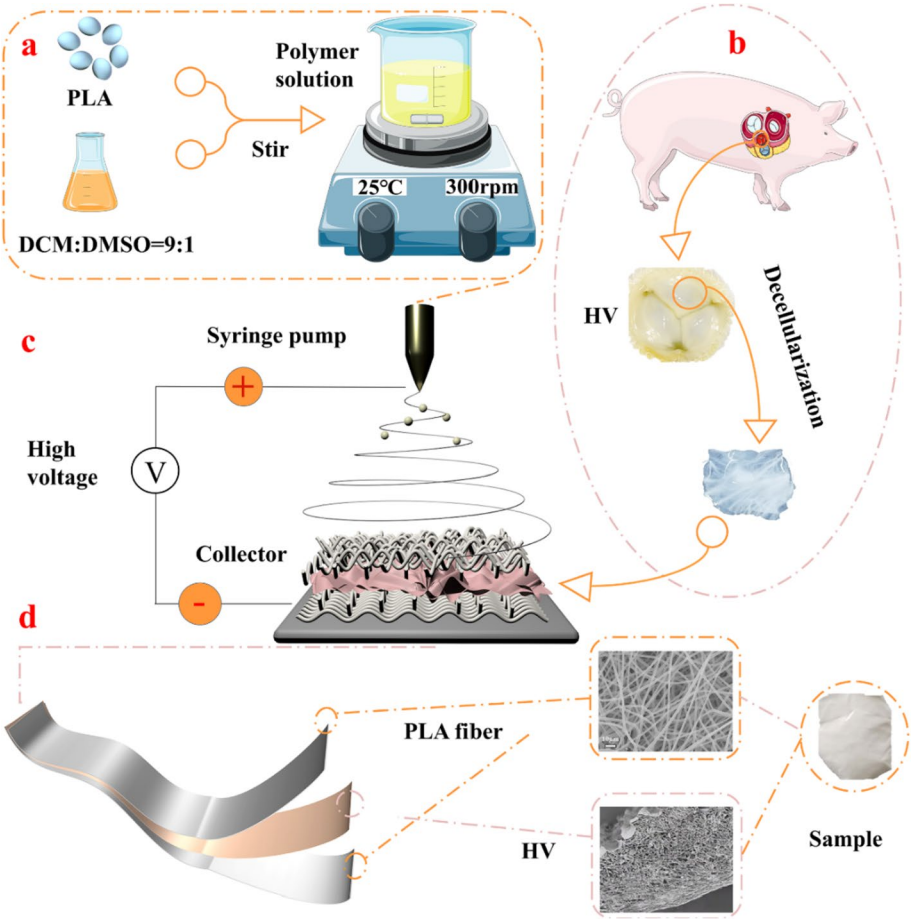

Fig. 1 Schematic illustration of PSES's preparation by electrospinning

Preparation of the PLA Electrospinning Solution

The polylactic acid particles were added in the solvent at a mass ratio of 10%, wherein the ratio of the solvent was DCM: DMSO=9:1. After magnetic stirring at room temperature for 4 h, a spinning solution was obtained for further use.

Preparation of Decellularized Heart Valves

The porcine aortic heart valves were removed under aseptic conditions, and the pig hearts were submerged in physiological saline containing sodium heparin. The swine aortic heart valves were shaken and rinsed in phosphate buffered saline (PBS) until no blood was visible on the surface of the heart valve. They were then put in high glucose Dulbecco's modified eagle medium (DMEM) medium containing antibiotics for 12 h at 4 °C. The heart valves were then surface decellularized with water-soluble and fat-soluble proteins, and

the heart valves were placed in groups with three parallels in six-well plates. Specific steps were as follows: [1] The porcine aortic heart valve was placed in a TRIS hydrochloride (TRIS-HCL) buffer (pH=7.8) with a concentration of 2% 3-propane sulfonate (CHAPS) and 2 mmol/L tributyl phosphate at room temperature for 24 h shaked on a shaker to obtain water-soluble decellularized porcine heart valve (W-DPHV). [2] W-DPHV was rinsed 6 times with deionized water, and each time more than 10 min was taken and was placed in TRIS-HCL buffer (pH=7.8) containing 2% CHAPS, 2 mmol/L tributyl phosphate, 1% amidosulfobetaine 14 (ASB-14), and 2% N-Decyl-N, N-dimethyl-3-ammonio-1-propane-sulfonate (SB3-10). W-DPHV was continued to be shaked at room temperature for 24 h to get a fat-soluble decellularized porcine heart valve (F-DPHV). [3] F-DPHV was taken out and rinsed with PBS for 4 times, each time was 6 h. It was then placed in TRIS-HCL buffer (pH=8) containing 1mmol/L $MgCl_2$ and 100 units/mL benzonase nuclease and continued to be shaked for 24 h at 37 °C to gain nuclear-soluble decellularized porcine heart valve (N-DPHV). [4] N-DPHV was rinsed for more than 4 times with PBS for 6 h each time. Finally, the decellularized porcine heart valve (DPHV) was obtained. The DPHV was placed in PBS containing antibiotics and stored at 4 °C for use.

Fabrication of the PLA Electrospun Scaffolds

The PLA electrospinning solution was imported into a 10 mL plastic syringe and spin using the electrospinning device. The spinning voltage was set to 18 kV, the injection distance was 15 cm, the injection speed was 1.5 mL/h, and the spinning humidity was about 45%. After the fibers were deposited for 30 min, 1, 2, and 3 h, the decellularized heart valve was flattened on a petri dish, fixed with forceps, and punctured with needles (about 30 times). The puncture-treated heart valve was laid flat on the center of the electrospinning membrane with continuously spinning. After spinning, the obtained membrane was placed in a vacuum oven at 40 °C and a vacuum of −0.1 to −0.05 MPa and dried for 12 h. The dried membrane was cut along the contour of the heart valve and separated from the aluminum foil to obtain an electrospun scaffold with a sandwich structure. Then, the product was placed in a PBS solution containing antibiotics and stored at 4 °C for use.

Characterization by Scanning Electron Microscopy (SEM)

The PSESs were lyophilized in a freeze dryer at −80 °C on the pressure of 5 Pa. Small pieces of the PSES were cut with a razor blade and attached to the electron microscope stage with conductive adhesive. The microscopic morphology of the samples was observed with a JSM-6700F scanning electron microscope (Electronics Co., Ltd, Japan). Electron microscope stage with the samples was sprayed with gold for 120 s and then placed under the electron microscope for observation. The fineness of the PLA electrospun fibers on the decellularized heart valve surface was then calculated and statistically analyzed using Image J image analysis software.

Fourier Transform Infrared Spectra Analysis of PSES

Fourier Transform Infrared analysis (FT-IR) was performed by a Tensor-27 Fourier transform infrared spectrometer (Bruker, Germany). The samples were tested with several parameters, of which the scanning range was 4000~600 cm^{-1}, the resolution was 8 cm^{-1},

the number of scans was 64, the test temperature was room temperature, and the method was attenuated total reflection.

Water Contact Angle of PSES

The electrospun scaffold with sandwich structure was taken out from PBS containing antibiotics, and the water on the surface was dried up with filter paper and then spread on a petri dish, placed in a −20 °C refrigerator, taken out after 10 h, and placed in the petri dish. Frozen samples and petri dish were lyophilized in a freeze dryer at −80 °C on the pressure of 5 Pa. The hydrophilicity and hydrophobicity of the electrospun scaffold surface were tested with a contact angle analyzer. The lyophilized samples were cut into small pieces and fixed on a glass slide to keep them flat. A total of 2 μL of distilled water was added dropwise with 5 to 7 parallels.

Softness of PSES

The electrospun scaffold of the sandwich structure was removed from the PBS containing antibiotics to keep the sample moist. The heart valve sample was clamped with a 5 mm tube clamp along the direction parallel to the warp yarn to keep a natural hanging state. Five samples were prepared for each group to be photographed at the same position and angle. Then, Image J image analysis software was used to calculate the overhanging angle of the heart valve. The calculation and analysis were performed based on the horizontal line, the intersection of the sample and the tube clamp, the angle formed by the sample, and the statistical angle, respectively.

Mechanical Properties of PSES

The electrospun scaffold membrane of the sandwich structure was cut into several parts along the longitudinal direction for strength test, of which the width was 5 mm. Six parallel samples for each group have been prepared. Tensile tests were performed by an Instron5943 Universal testing machine with a 10 N sensor, 50 N grips, a set grip spacing of 8 mm, and a fixed speed of 5 mm/min. Following the completion of the test, a drawing analysis of their mechanical properties was performed.

Thermal Properties of PSES

Differential scanning calorimetry (DSC) studies of the electrospun scaffold membrane of the sandwich structure were conducted on a DSCQ2000 (TA Instruments, USA) under N_2 at a temperature ranging of 0–200 °C with the increase rate of temperature set at 10 °C/min. The preparation of samples involved cutting the electrospun scaffold into pieces with weights ranging from 5 to 10 mg.

In Vitro Cell Experiment

HUVECs were kindly provided by Union Hospital Affiliated to Tongji Medical College, Huazhong University of Science and Technology. The cells were cultured at 37 °C in Dulbecco's Modified Eagle Media (DMEM, Gibco) with 10% fetal bovine serum (FBS,

Gibco) in a humidified incubator with 5% CO_2. When the density of cell proliferation in the culture plate (25 cm^2, Corning) reached 80–90%, the cells were digested with 0.25 % trypsin (1 mL) and then resuspended in culture medium. Subsequently, cells were cultured until passaged to 3–5 generations. The growth cycle and morphology of the HUVECs were observed by CKX41 inverted microscope (OLYMPUS, Japan) and EVOS M500 cell imaging system (Invitrogen, USA), respectively.

Cell Adhesion

The electrospun scaffold with sandwich structure was prepared with diameters of 24 mm matching the 6-well plates (Corning). Thereafter, the samples were sterilized in 3 mL purified water with 0.1% (v/v) peracetic acid solution Aqueous One Solution for 3 h and washed with PBS. Subsequently, the cell suspension (200 μL) was seeded on each sample at a density of 1×10^5 cells/mL and co-cultured for 3 h. In brief, at periodic intervals, the samples were washed with PBS and incubated with 150 μL culture medium and 15 μL CCK-8 for 2 h. A total of 100 μL suspension was collected and placed in new 96-well plates. The optical density (OD) value of the suspension at 450 nm in each well was measured by an Enzyme Microplate Reader (Thermo Fish Scientific, USA). Four parallels in each group were tested ($n = 4$).

Cell Proliferation

Living cells were determined at 1, 3, and 5 days by cell proliferation assay according to the manufacturer's protocol. The number of cells on the surface of the electrospun scaffold was determined in real time by the cell adhesion method using CCK-8. The OD value of the media was measured at 450 nm using a microplate reader. Four parallels in each group were tested ($n = 4$).

Cell Viability of PSES

The cell suspension (200 μL) was first seeded on the prepared and sterilized electrospun scaffold for the cell viability test at a density of 1×10^5 cells/mL. After cultured for 1, 3, and 5 days, the cell viability of PSES was stained with the Calcein-AM/PI double staining kit (BestBio, China). The cells were observed with a cell imaging system to detect living cells (stained by Calcein-AM, green fluorescence) and dead cells (stained by PI, red fluorescence). The number of live and dead cells was counted using Image J in each sample, and the live ratio was calculated by the number of living cells divided by the total number of cells.

Cell Morphology After Cultured for 1 Day

After cultured for 1, 3, and 5 days, the culture medium was removed, and the cells were stained with 1 μg/mL F-actin phalloidin (Yisheng Bio-Technology Co., Ltd., Shanghai) for 30 min and 10 μg/mL 4,6-diamidino-2-phenylindole, dihydrochloride (DAPI, Beijing Labgic Technology Co., Ltd.) for 5 min. The cells were observed with a cell imaging system to detect the cell skeleton (stained by F-actin phalloidin, green fluorescence) and the nucleus (stained by DAPI, blue fluorescence).

Statistical Analysis

Statistics were performed with GraphPad Prism 8.3 software (GraphPad Software, San Diego, California). All data were represented as mean values ± standard deviation (SD, $n \geq 3$). The statistical significance was determined using two-tailed Student's test ($^{*}p<0.05$, $^{**}p<0.01$) unless otherwise stated.

Results and Discussion

Fabrication and Characterization of PLA Electrospun Scaffolds

In this paper, PLA sandwich structure electrospun scaffold (PSES) was obtained by decellularizing porcine valves as heart valve scaffold cores, which were subsequently used as PLA coverings for superficial structures. After puncture treatment and electrostatic spinning, the different thicknesses of PSES were investigated, which were obtained by electrostatic spinning at different times. The scaffold composed of electrospun as the surface layer and decellularized heart valve as the core layer was shown in the heart valve after puncture treatment was flattened in the center of the electrospinning fiber. After different times, electrospinning scaffolds with different thicknesses were obtained.

To enhance the mechanical properties of decellularized porcine valves and to provide a more suitable three-dimensional environment for cell growth, electrospinning was used to cover the surface of the decellularized heart valve with PLA. The surface and cross-section of PSES and DHV were characterized by SEM (Fig. 2A). The surface departs the extracellular substrate after decellularization, and the membrane interface has a nest-shaped porous structure. In the surface images of PSES, PLA fibers could be seen on the surface of the decellularized heart valve layer, which proved that there was a certain adhesion between the decellularized heart valve and the PLA electrospinning membrane. The outer

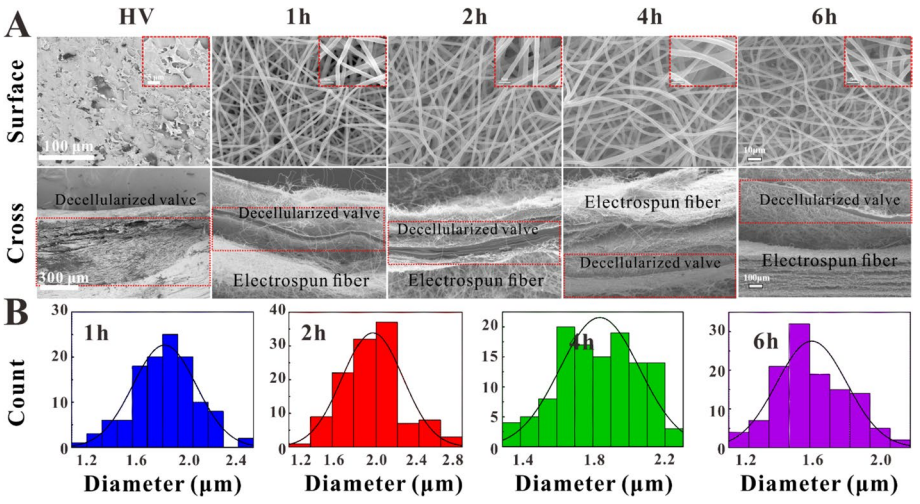

Fig. 2 SEM of the surface and the cross-section morphology of DHV and PSES at 1, 2, 4, and 6 h (**A**); the surface fiber diameter distribution of PSES (**B**)

synthetic fabric was of uniform thickness and was tightly attached to the inner tissue, as indicated by the thin interface between layers. Pingli Wu et al. reported that to provide a snug-fitting fibrous tissue layer, a hybrid small-diameter catheter consisting of electrostatically spun wire-coated polyurethane wrapped around decellularized aortic intima was also employed. The decellularized heart valve was shown in cross-sectional PSES images to be sandwiched between two layers of PLA electrospun fiber membranes. The thickness of the PLA electrospun film increases with increasing electrospinning time, indicating the electrospinning time could be changed to alter the scaffold's thickness. It is important to note that after 6 h of electrospinning, the PLA electrospinning film showed apparent signs of delamination. This delamination may have resulted from the electrostatic spinning film's increased thickness, which suggests that the electrospinning period should not be excessive. Following quantitative analysis, all of the photos demonstrated that PLA fibers were uniformly fine after 1, 2, 4, and 6 h of electrospinning (Fig. 2B). The fibers on the surface of the decellularized heart valve were mainly concentrated at 1.8, 2.0, 1.9, and 1.6 μm, when the spinning time was 1, 2, 4, and 6 h, suggesting that changing the spinning time would not have a significant impact on the fiber surface structure while keeping other electrospinning process parameters constant. Based on earlier research, the 1.8 μm PLA fiber diameter was chosen for its high cell viability [26]. As a result, the sandwich-shaped electrospun scaffold made from PLA had a stable surface microstructure.

For group structure analysis, qualitative and quantitative analysis of compound materials, FT-IR analysis was used to investigate decellularized porcine heart valve treated with different electrospinning times. Decellularized heart valves after electrospinning for 1, 2, 4, and 6 h were tested, and pure PLA membrane was the control (Fig. 3A). The absorption bands at 1182 cm^{-1} and 1091 cm^{-1} correspond to the stretching mode of C-O-C and C-C functional groups [27, 28], the symmetric and asymmetric stretching, respectively. The spectral band at 921 cm^{-1} which could confirm the formation of α crystals was not found; this might be due to the lower crystallinity of electrospun PLA films [29]. Furthermore, the corresponding peaks of the spectra of the decellularized heart valves with different electrospinning times were completely consistent with those of pure PLA membranes. Additionally, the absorption bands at 1380 cm^{-1} and 1761 cm^{-1} in the spectra of the decellularized porcine heart valve without electrospinning (HV) were due to the stretching vibration of

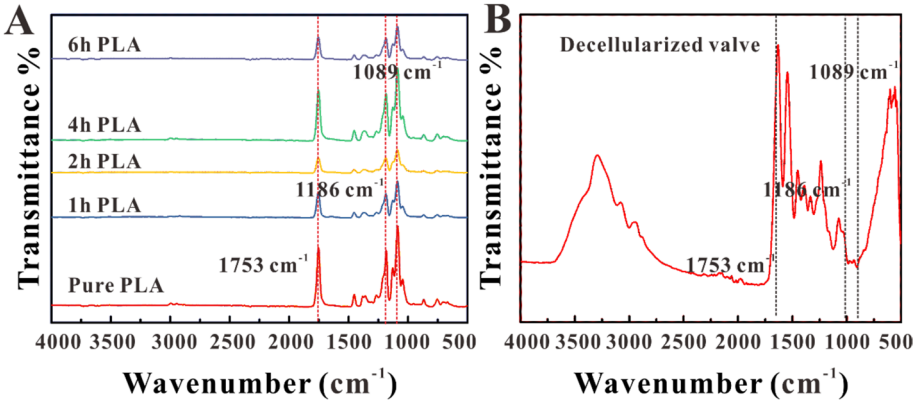

Fig. 3 The FT-IR spectra of PSES and pure PLA membrane after 1, 2, 4, and 6 h PLA electrospinning treatment (**A**); the FT-IR spectra of decellularized porcine heart valve without electrospinning (**B**)

-CH- and the -C=O bond in PLA (Fig. 3B), respectively. It could be seen that the absorption bands in spectra at 1089 cm^{-1}, 1186 cm^{-1}, and 1753 cm^{-1} were completely inconsistent with the spectra of the decellularized porcine heart valve treated with PLA. The aforementioned findings show that, depending on the electrospinning period, PLA fibers could completely cover the decellularized pig heart valve.

The contact angle of the decellularized porcine heart valve treated with different electrospinning times was characterized (Figure S1). Decellularized porcine heart valve surfaces' contact angles were 120.85 ± 1.17°, 120.05 ± 1.4°, 125.68 ± 1.71°, and 132.73 ± 1.69°with hydrophobic structures, respectively. This indicated that the hydrophobic properties of the PSES surface had not changed, and the contact angles were all greater than 120°. These could be the cause of the other surface PLA electrospinning process parameters, with the exception of the spinning time, remaining unaltered. The sandwich structure electrospun scaffold was able to achieve stability of the surface structure with stable hydrophilic and hydrophobicity, as evidenced by the measured hydrophilic and hydrophobicity of the surface, which matched those of surface-covered electrospun polylactic acid film.

Thermal Properties of PLA Electrospun Scaffolds

The thermal stability of decellularized porcine heart valve treated with different electrospinning times was investigated. After heating scan of PSESs with different electrospinning times, DSC curves were obtained with pure PLA as the control (Fig. 4A). The results of quadrant II of DSC curves showed the melting temperatures of PSES and pure PLA at different times were 161.53 °C, 162.01 °C, 162.07 °C, 162.18 °C, and 161.83 °C (Fig. 4B), which was consistent with melting peaks of pure PLA in previous work [30]. The results of quadrant I of DSC curves showed the cold crystallization temperature (Tc) of PSESs was 76.18 °C, 88.11 °C, and 87.57 °C, and melting point (Tm) was 60.81 °C, 61.36 °C, and 63.48 ° (Fig. 4C). The Tc of PLA film was 86.4 °C, which was within the range of glass transition temperature (Tg, 40–70 °C) and the Tm (130–230 °C or typical 170–180 °C) of PLA reported in the literature [31]. Around 60 °C, which corresponds to the densification of the glassy amorphous chains of PLA during physical aging, is where the endothermic peaks with the glass transition of PLA and its nanocomposites overlap. This may be because molecular rearrangements encouraged thermodynamic variables to move towards equilibrium value. With longer electrospinning times, a little rise in Tg, Tc, and Tm was seen. The thermal characteristics of electrospun PLA were somewhat altered as expected by the different electrospinning times.

Furthermore, XRD of decellularized porcine heart valve without electrospinning, pure PLA, and PSESs were characterized. The results showed the typical characteristic peak of heart valve at ~16.60° and pure PLA at ~22.52° in PLA electrospun scaffolds (Fig. 4D), indicating that these PSESs were a mixture of amorphous and crystalline phases and that no secondary phase was produced during the synthesis [32]. Additionally, it was discovered that as the electrospinning duration increased, the PLA phase's signal became more pronounced and the decellularized porcine heart valve's diffraction peaks became weaker, which was consistent with the steady rise in PLA content.

Mechanical Properties of PLA Electrospun Scaffolds

Heart valves in our bodies encounter a variety of complex mechanical forces. Uniaxial tensile testing was widely used to characterize native heart valve tissue as well as biological

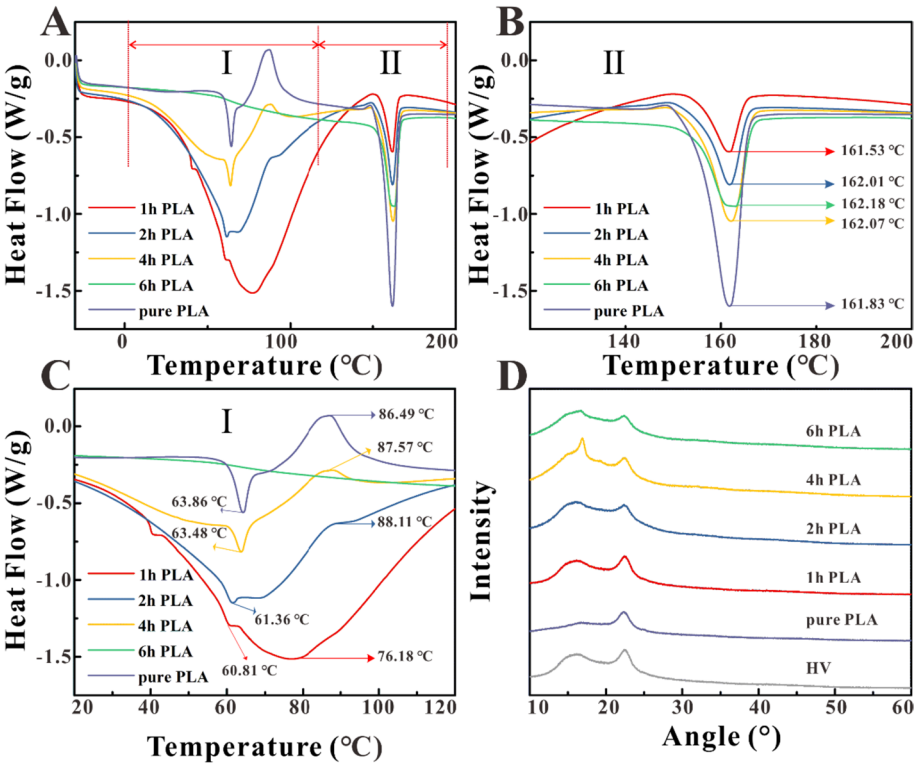

Fig. 4 The DSC curves of PSESs treated with different electrospinning times at 1, 2, 4, and 6 h (**A**), partial enlargements of quadrant II (**B**) and quadrant I (**C**) in **A**; XRD spectra of decellularized porcine heart valve without electrospinning (gray), pure PLA (purple) and 1 h (red), 2 h (blue), 4 h (yellow), and 6 h (green) of PSESs (**D**)

prostheses in clinical, so that the results could be used as a benchmark for the development of scaffolds in HVTE [33–36]. To analyze the mechanical properties of PSESs affected by the thickness of PLA, uniaxial tensile tests were performed (Fig. 5). With the electrospinning time, the results of the stress-strain curve showed the strength and tensile deformation gradually increased (Fig. 5A). At 6 h of the electrospinning time, the result showed the strength was 2–6.5 N, the tensile deformation was between 150 and 400%, and the elastic modulus reached 15 MPa (Fig. 5B–D). According to previous works, the pressure on the heart valve should be 2–6 kpa when the flow rate was 2.5–4.5 L/min [37]. As the electrostatic spinning period lengthens, the resulting support becomes thicker. These tensile mechanical test findings showed that the heart valve's thickness expanded over time while its mechanical characteristics also greatly improved. As a result, we could control the mechanical characteristics of the heart valve by varying the length of the electrospinning time to suit needs.

The PSESs manufactured in the wet state with various electrospinning times had their bending degrees measured (Fig. 6A–D). According to the findings, the angles of PSESs with electrospinning times of 1, 2, 4, and 6 h were 54.47 ± 7.60°, 43.96 ± 1°, 26.63 ± 6.57°, and 16.66 ± 4.45°, respectively. The degree of the control, a decellularized porcine heart valve in the wet state without electrospinning, was 90°(Fig. 6E). The degree of crook

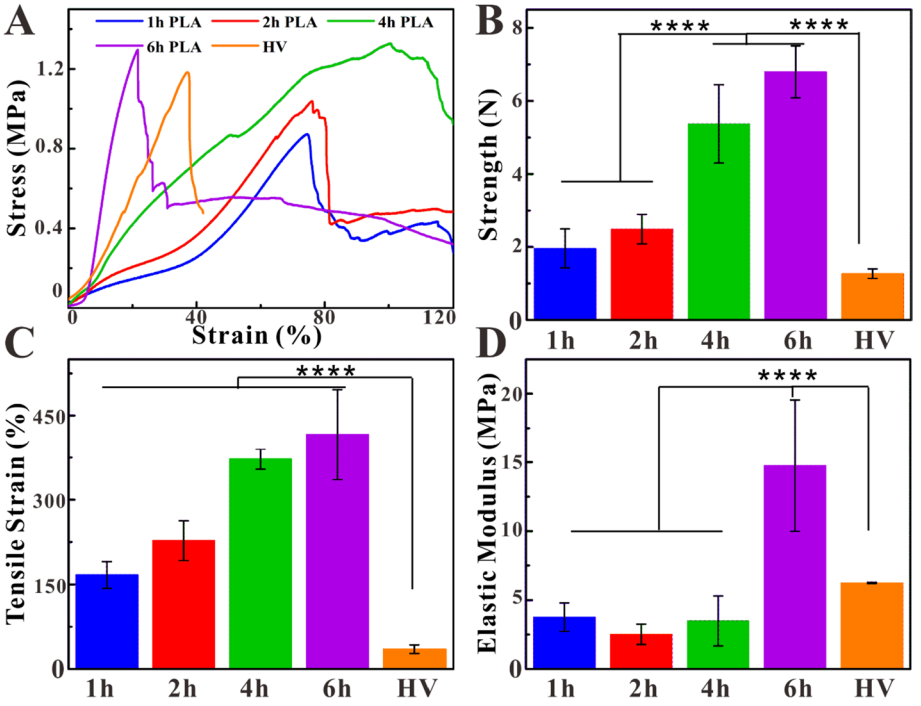

Fig. 5 Mechanical properties with stress-strain curve (**A**); strength (**B**), tension elongation (**C**); the elastic modulus (**D**) of PSESs treated with different electrospinning times (n=6)

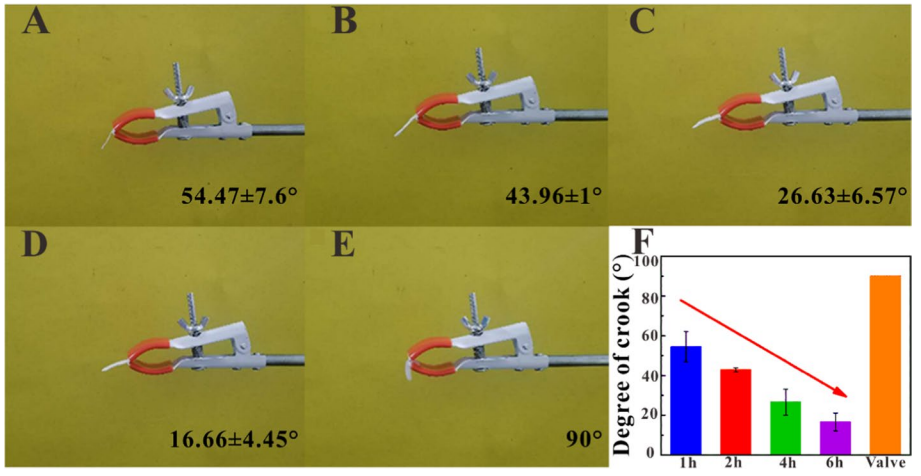

Fig. 6 The bending degree of the decellularized porcine heart valve in the wet state treated with different electrospinning times at 1 (**A**), 2 (**B**), 4 (**C**), and 6 h (**D**); the bending degree of the decellularized porcine heart valve without electrospinning (**E**); the quantitative analysis (**F**) of **A**–**E** (n=5)

histogram revealed that as the length of the electrospinning time increased, the samples' degree of bending shrank and shrank with the length of the electrospinning time (Fig. 6F). The amount of bending after coming into contact with water revealed how fragile the heart valve was. As a result, everything said above suggested that by adjusting the electrospinning duration, the softness of the heart valve could be easily altered.

Biocompatibility and In Vivo Cell Behaviors

Cell adhesion on the surface of the sandwich structure electrospun scaffolds treated with different electrospinning times was tested by CCK-8 (Fig. 7A). The results showed there were significantly more cells adhered to the surface of HV compared with the PSESs treated with PLA electrospinning (*p<0.05). In addition, there were no significant differences between the adhesion performances of the sandwich structure electrospun scaffolds treated with electrospinning at 1, 2, 4, and 6 h. It was because the decellularized porcine heart valve was a natural biomaterial with excellent cytocompatibility, of which cell adhesion ability was significantly better than that of the PLA electrospun membrane as the scaffold on the surface. While DHV offers good short-term cell compatibility, composite shelves with larger rooms have higher cell compatibility for long-term cell development. The cell culturing cycle is longer, and time is more pressing. Thus, comparisons between the experimental group and the control group can also reflect good cellular compatibility of PSESs in the short and long term.

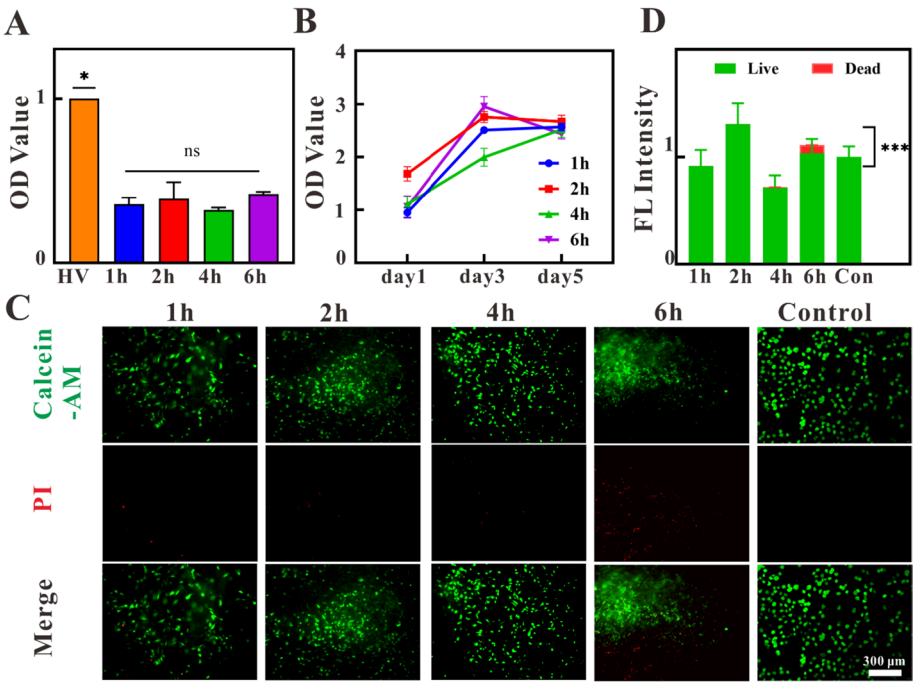

Fig. 7 Cell adhesion (**A**) of HUVECs incubated with PSESs treated with different electrospinning times after 4 h, cell proliferation (**B**), cell viability (**C**), and the quantitative analysis of fluorescence-stained bone cell viability (**D**) of HUVECs incubated with PSESs treated with different electrospinning times after 24 h

The cell proliferation of cells on the surface of the sandwich structure electrospun scaffolds treated with different electrospinning times at 1, 3, and 5 days were investigated by the CCK-8 tests (Fig. 7B). According to the findings, cells on both the PSES and the decellularized porcine heart valve proliferated quite effectively at 1–3 days. The results showed that, on the 5th day, the number of cells on the PSESs that had been electrospun for 6 h had dramatically decreased, whereas the number of cells on the other samples had stabilized. The multilayer PLA electrospinning membrane hampered the delivery of nutrients to the cells in the medium, causing some cells to undergo apoptosis, and the surface of the sample was entirely covered with proliferating cells after being cultured for 5 days. These factors were the causes of the decreasing trend.

After being treated with the PSESs, HUVECs were stained with green fluorescent calcein (AM) and red fluorescent propyliodide (PI), respectively, to distinguish between living and dead cells (Fig. 7C). As seen, a significant amount of green fluorescence occurred in the cells incubated with PSESs for 1, 2, and 4 h of electrospinning, indicating that there are more live cells. As can be observed in the image, there are much less viable cells on the surface of the electrospun scaffolds when the electrospinning time is 6 h. Combined with the quantitative analysis of the fluorescence-stained bone cell viability (Fig. 7D), the results demonstrated that the PSES with electrospinning at 2 h expressed the largest living cell fluorescence compared with the other electrospinning time of PSES.

These findings showed that the electrospun scaffolds electrospun for 1, 2, and 4 h had good biocompatibility and cell-growth-friendly surfaces. The 2 h PSES group may offer a favorable environment that will encourage the growth and division of live cells. The PLA coating on the surface of the decellularized porcine heart valve was too thick when the electrospinning period was 6 h, which caused an evident delamination effect and inhibited cell development.

HUVECs were stained with F-actin phalloidin and DAPI fluorescent in order to observe the morphological alterations of the HUVECs cultured with PSESs treated with various electrospinning times (Fig. 8). The findings revealed that HUVECs had a polygonal cell

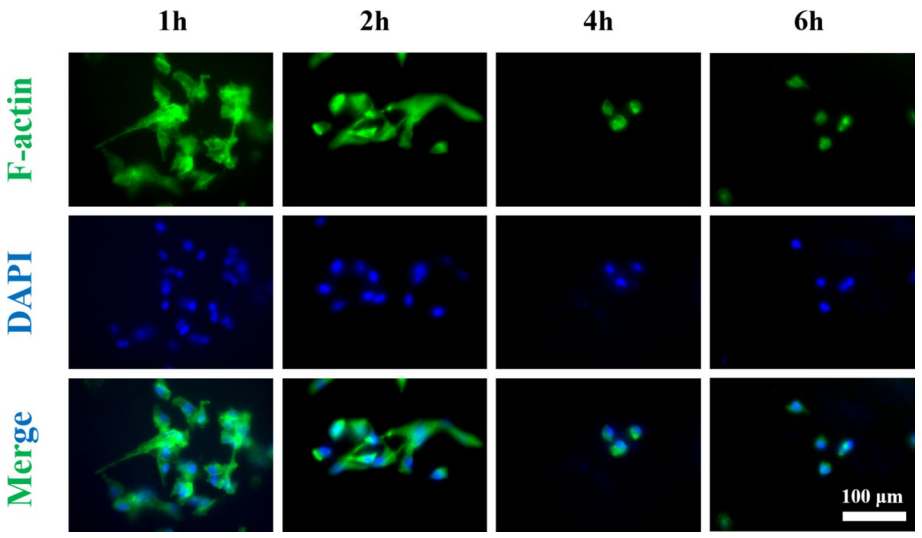

Fig. 8 Cell morphology of HUVECs incubated with PSESs treated with different electrospinning times after 24 h

morphology on the electrospun scaffold after 1 and 2 h of electrospinning, indicating that the cells might spread out entirely and had a clear propensity to do so. However, HUVECs on the electrospun scaffold surface after 4 and 6 h of electrospinning displayed a clumped distribution with an oval cell shape and were not completely dispersed. According to the findings, if the electrospinning time was too long, the PLA electrospinning film on the surface of the decellularized porcine heart valve was too thick, resulting in delamination and other phenomena that affected the migration behavior of cells and affected their biocompatibility.

Conclusion

In this study, decellularized heart valve and PLA were employed as raw materials in the electrospinning method to create a sandwich-shaped electrospun scaffold. The next conclusions were reached: [1] The change in electrospinning time would not have a significant impact on the physicochemical characteristics of the decellularized porcine heart valve surface. [2] The thickness of the electrospun scaffold could be adjusted by changing the electrospinning time. [3] The longer the electrospinning time, the greater the strength and tensile strain, and the stiffer the heart valve scaffold would be. [4] When the electrospinning time was too long, the stiffness of the heart valve scaffold would also significantly increase. In conclusion, electrospinning for 2 h can produce a biological heart valve with specific biomechanical features and strong biocompatibility. It gave researchers an approach that seemed promising for creating tissue-engineered heart valves that could eventually satisfy the needs of heart valves for replacement, regeneration, and growth.

Supplementary Information The online version contains supplementary material available at https://doi.org/10.1007/s12010-023-04756-8.

Author Contributions Chaorong Wang: conceptualization, methodology, data curation, software, writing—original draft preparation, formal analysis.
Qingqing Chen: conceptualization, data curation.
Han Wang: visualization, methodology, writing—original draft preparation, formal analysis.
Hanlin Gang: conceptualization, methodology, writing—original draft preparation.
Yingshan Zhou: writing—reviewing and editing.
Shaojin Gu: writing—reviewing and editing.
Ruoyun Zhang: writing—reviewing and editing, investigation, project administration.
Weilin Xu: investigation, funding acquisition.
Hongjun Yang: conceptualization, writing—reviewing and editing, supervision, investigation, funding acquisition, project administration.
All authors read and approved the final manuscript.

Funding This work was supported by the Natural Science Foundation of Hubei Province (No. 2020CFA022) and the Key Research and Development Program of Hubei Province (No.2022ACA002).

Data Availability Data are available on request from the authors. The data that support the findings of this study are available from the corresponding author upon reasonable request.

Declarations

Ethical Approval Not applicable

Consent to Participate Not applicable

Consent for Publication Not applicable

Conflict of Interest The authors declare no competing interests.

References

1. Kostyunin, A. E., Yuzhalin, A. E., Rezvova, M. A., Ovcharenko, E. A., Glushkova, T. V., & Kutikhin, A. G. (2020). Degeneration of bioprosthetic heart valves: Update 2020. *Journal of the American Heart Association, 9*, e018506.
2. Sellers, S. L., Turner, C. T., Sathananthan, J., Cartlidge, T. R. G., Sin, F., Bouchareb, R., Mooney, J., Norgaard, B. L., Bax, J. J., Bernatchez, P. N., Dweck, M. R., Granville, D. J., Newby, D. E., Lauck, S., Webb, J. G., Payne, G. W., Pibarot, P., Blanke, P., Seidman, M. A., & Leipsic, J. A. (2019). Transcatheter aortic heart valves: Histological analysis providing insight to leaflet thickening and structural valve degeneration. *JACC: Cardiovascular Imaging, 12*, 135–145.
3. Alkhouli, M., Alqahtani, F., Simard, T., Pislaru, S., Schaff, H. V., & Nishimura, R. A. (2021). Predictors of use and outcomes of mechanical valve replacement in the United States (2008-2017). *Journal of the American Heart Association, 10*, e019929.
4. Goldstone, A. B., Chiu, P., Baiocchi, M., Lingala, B., Patrick, W. L., Fischbein, M. P., & Woo, Y. J. (2017). Mechanical or biologic prostheses for aortic-valve and mitral-valve replacement. *New England Journal of Medicine, 377*, 1847–1857.
5. Rodriguez-Gabella, T., Voisine, P., Puri, R., Pibarot, P., & Rodes-Cabau, J. (2017). Aortic bioprosthetic valve durability: Incidence, mechanisms, predictors, and management of surgical and transcatheter valve degeneration. *Journal of the American College of Cardiology, 70*, 1013–1028.
6. Usprech, J., Romero, D. A., Amon, C. H., & Simmons, C. A. (2017). Combinatorial screening of 3D biomaterial properties that promote myofibrogenesis for mesenchymal stromal cell-based heart valve tissue engineering. *Acta biomaterialia, 58*, 34–43.
7. Yan, G., Liu, Y., Xie, M., Shi, J., Qiao, W., Dong, N., Wq, G., Yl, M., Js, W., & Nd. (2021). Experimental and computational models for tissue-engineered heart valves: A narrative review. *Biomaterials Translational, 2*, 361–375.
8. VeDepo, M. C., Detamore, M. S., Hopkins, R. A., & Converse, G. L. (2017). Recellularization of decellularized heart valves: Progress toward the tissue-engineered heart valve. *Journal of tissue engineerin, 8*, 2041731417726327.
9. Boroumand, S., Asadpour, S., Akbarzadeh, A., Faridi-Majidi, R., & Ghanbari, H. (2018). Heart valve tissue engineering: An overview of heart valve decellularization processes. *Regenerative medicine, 13*, 41–54.
10. Ott, H. C., Matthiesen, T. S., Goh, S.-K., Black, L. D., Kren, S. M., Netoff, T. I., & Taylor, D. A. (2008). Perfusion-decellularized matrix: Using nature's platform to engineer a bioartificial heart. *Nature medicine, 14*, 213–221.
11. Rieder, E., Kasimir, M.-T., Silberhumer, G., Seebacher, G., Wolner, E., Simon, P., & Weigel, G. (2004). Decellularization protocols of porcine heart valves differ importantly in efficiency of cell removal and susceptibility of the matrix to recellularization with human vascular cells. *The Journal of thoracic and cardiovascular surgery, 127*, 399–405.
12. Schmidt, D. (2007). Stock UA Hoerstrup SP. *Philosophical Transactions of the Royal Society, 362*, 1505–1512.
13. Yacoub, M. T. J. J. *Will heart valve tissue engineering change the world* (pp. 60–61).
14. Stella, J. A. and Sacks, M. S. (2007) On the biaxial mechanical properties of the layers of the aortic valve leaflet.
15. Nemavhola, F. (2021). Study of biaxial mechanical properties of the passive pig heart: Material characterisation and categorisation of regional differences. *International Journal of Mechanical and Materials Engineering, 16*.
16. Wen, S., Qiao, W., Zhang, Y., & Dong, N. (2020). Development and trend in the field of valvular heart disease in China: An analysis based on the National Natural Science Foundation of China. *Annals of Translational Medicine, 8*, 449.
17. Dai, J., Qiao, W., Shi, J., Liu, C., Hu, X., & Dong, N. (2019). Modifying decellularized aortic valve scaffolds with stromal cell-derived factor-1alpha loaded proteolytically degradable hydrogel for recellularization and remodeling. *Acta Biomaterialia, 88*, 280–292.
18. Bahremandi-Toloue, E., Mohammadalizadeh, Z., Mukherjee, S., & Karbasi, S. (2022). Incorporation of inorganic bioceramics into electrospun scaffolds for tissue engineering applications: A review. *Ceramics International, 48*, 8803–8837.
19. Del Gaudio, C., Grigioni, M., Bianco, A., & De Angelis, G. (2008). Electrospun bioresorbable heart valve scaffold for tissue engineering. *International Journal of Artificial Organs, 31*, 68–75.

20. Eslami, M., Vrana, N. E., Zorlutuna, P., Sant, S., Jung, S., Masoumi, N., Khavari-Nejad, R. A., Javadi, G., & Khademhosseini, A. (2014). Fiber-reinforced hydrogel scaffolds for heart valve tissue engineering. *Journal of biomaterials application, 29*, 399–410.
21. Sant, S., Iyer, D., Gaharwar, A. K., Patel, A., & Khademhosseini, A. (2013). Effect of biodegradation and de novo matrix synthesis on the mechanical properties of valvular interstitial cell-seeded polyglycerol sebacate–polycaprolactone scaffolds. *Acta biomaterialia, 9*, 5963–5973.
22. Shinoka, T. (2015). Current status of cardiovascular tissue engineering. *International Journal of Clinical Therapeutics and Diagnosis, 3*, 1–10.
23. Ye, K., Liu, D., Kuang, H., Cai, J., Chen, W., Sun, B., Xia, L., Fang, B., Morsi, Y., & Mo, X. (2019). Three-dimensional electrospun nanofibrous scaffolds displaying bone morphogenetic protein-2-derived peptides for the promotion of osteogenic differentiation of stem cells and bone regeneration. *Journal of colloid and interface science, 534*, 625–636.
24. Mohammadalizadeh, Z., Bahremandi-Toloue, E., & Karbasi, S. (2022). Synthetic-based blended electrospun scaffolds in tissue engineering applications. *Journal of Materials Science, 57*, 4020–4079.
25. Imani, F., Karimi-Soflou, R., Shabani, I., & Karkhaneh, A. (2021). PLA electrospun nanofibers modified with polypyrrole-grafted gelatin as bioactive electroconductive scaffold. *Polymer, 218*.
26. Herrero-Herrero, M., Alberdi-Torres, S., González-Fernández, M. L., Vilariño-Feltrer, G., Rodríguez-Hernández, J. C., Vallés-Lluch, A., & Villar-Suárez, V. (2021). Influence of chemistry and fiber diameter of electrospun PLA, PCL and their blend membranes, intended as cell supports, on their biological behavior. *Polymer Testing, 103*.
27. Li, T., Liu, Y., Qin, Q., Zhao, L., Wang, Y., Wu, X., & Liao, X. (2021). Development of electrospun films enriched with ethyl lauroyl arginate as novel antimicrobial food packaging materials for fresh strawberry preservation. *Food Control, 130*.
28. Nizamuddin, S., Hossain, N., Qureshi, S. S., Al-Mohaimeed, A. M., Tanjung, F. A., Elshikh, M. S., Siddiqui, M. T. H., Baloch, H. A., Mubarak, N. M., Griffin, G., & Srinivasan, M. (2021). Experimental investigation of physicochemical, thermal, mechanical and rheological properties of polylactide/rice straw hydrochar composite. *Journal of Environmental Chemical Engineerin, 9*.
29. Beltrán, F. R., de la Orden, M. U., Lorenzo, V., Pérez, E., Cerrada, M. L., & Martínez Urreaga, J. (2016). Water-induced structural changes in poly(lactic acid) and PLLA-clay nanocomposites. *Polymer, 107*, 211–222.
30. Lopresti, F., Campora, S., Tirri, G., Capuana, E., Carfi Pavia, F., Brucato, V., Ghersi, G., & La Carrubba, V. (2021). Core-shell PLA/Kef hybrid scaffolds for skin tissue engineering applications prepared by direct kefiran coating on PLA electrospun fibers optimized via air-plasma treatment. *Materials Science and Engineering: C, 127*, 112248.
31. Fan, T., & Daniels, R. (2021). Preparation and characterization of electrospun polylactic acid (PLA) fiber loaded with birch bark triterpene extract for wound dressing. *AAPS PharmSciTech, 22*, 205.
32. Ke, W., Li, X., Miao, M., Liu, B., Zhang, X., & Liu, T. (2021). Fabrication and properties of electrospun and electrosprayed polyethylene glycol/polylactic acid (PEG/PLA) films. *Coatings, 11*.
33. Balguid, A., Rubbens, M. P., Mol, A., Bank R. A, Bogers, A. J., van Kats, J. P., de Mol, B. A., Baaijens, F. P., & Bouten, C. V. (2007). The role of collagen cross-links in biomechanical behavior of human aortic heart valve leaflets--Relevance for tissue engineering. *Tissue engineering, 13*, 1501–1511.
34. Kalejs, M., Stradins, P., Lacis, R., Ozolanta, I., Pavars, J., & Kasyanov, V. (2009). St Jude Epic heart valve bioprostheses versus native human and porcine aortic valves - Comparison of mechanical properties. *Interactive cardiovascular and thoracic surgery, 8*, 553–556.
35. Saidy, N. T., Wolf, F., Bas, O., Keijdener, H., Hutmacher, D. W., Mela, P., & De-Juan-Pardo, E. M. (2019). Biologically inspired scaffolds for heart valve tissue engineering via melt electrowriting. *Small, 15*, e1900873.
36. Stradins, P., Lacis, R., Ozolanta, I., Purina, B., Ose, V., Feldmane, L., & Kasyanov, V. (2004). Comparison of biomechanical and structural properties between human aortic and pulmonary valve. *European Journal of Cardio-thoracic Surgery, 26*, 634–639.
37. Hatoum, H., & Dasi, L. P. (2019). Reduction of pressure gradient and turbulence using vortex generators in prosthetic heart valves. *Annals of biomedical engineering, 47*, 85–96.